PLS0009

Land Surface Temperature Estimation for Buriram Town Municipality, Thailand

Pantip Piyatadsananon[1,*] and Ekkaluk Salakkham[1]

[1]School of Geoinformatics, Institute of Science, Suranaree University of Technology, University Avenue Muang District, Nakhon Ratchasima, 30000, Thailand.

* Corresponding Author: pantip.p@sut.ac.th

Abstract. Land Surface Temperature (LST) has long been monitored and studied; however, the most reliable method of estimating the LST has yet to be examined regarding the mixed land-use types over a small city. This research explores an optimum method for Land Surface Temperature (LST) estimation in a city using the data from LANDSAT-8. Four favored LST retrieval approaches, the Radiative Transfer Equation-based method (RTE), the Improved Mono-Window method (IMW), the Generalized Single-Channel method (GSC), and the Split-Window algorithm (SW), were used to estimate the LST over Buriram Town Municipality, Thailand. The calculated LST from these four methods were compared with ground-based temperature data of 100 measured sites over the study area on the same date and time of the employed Landsat-8 data. The lowest Normalized Root Means Square Error (NRMSE) was considered to identify the optimum method of the LST estimation. The SW algorithm provides the lowest NRMSE value (0.114), followed by the RTE (0.171), the IMW algorithm (0.181), and the GSC (0.219). As a result, the SW algorithm is the optimum method in LST estimation for Buriram Town Municipality. The SW algorithm mainly eliminates atmospheric effects based on differential absorption in two thermal bands, which have shown the smallest error in the retrieval of LST. The explored optimal method will benefit GIS specialists working for Buriram local government to conduct the best practice to monitor the LST over the city. The other local governments could consider the SW algorithm to monitor the LST over their small cities with similar contents
.

Keywords. Split-window; LANDSAT-8; Land Surface Temperature (LST); Thermal bands; Buriram**.**

1. Introduction

Land Surface Temperature (LST) is an essential variable for estimating radiation and energy budgets associated with mainland surface processes [1-3]. Knowledge of LST distribution can provide useful information about the surface's physical properties and climate, which have a role in a variety of fields, including land-atmosphere energy budget [4, 5], climate change [5-7], hydrological cycle [5, 7, 8], evapotranspiration [6, 8], and urban climate [4, 8, 9]. LST data from satellite remote sensing provides denser spatial sampling intervals than those taken at ground sites [10]. Data from the LANDSAT series is widely used for retrieving the LST, according to the downloadable free data from the USGS website, regular revisit times, and long-term recorded data captured by two on board instruments: the Operational Land Imager (OLI) and the Thermal Infrared Sensor (TIRS) [11]. Based on the TIR bands of Landsat-8, the available data is appropriate to apply the split-window algorithms (SW) [12] and three LST estimation methods of single-channel methods, Radiative Transfer Equation-based method (RTE), the Improved Mono-Window method (IMW), and the Generalized Single-Channel method (GSC) [13]. Weng *et al.* [14] indicated that the estimation of emissivity for ground objects from passive sensor data could be measured using different technics. Liu *et al.* [15] and Coll *et al.* [16] noted that LST estimation was performed over the large fully vegetated surface, bare surfaces, and deserts, with relatively homogeneous test sites avoiding uncertainty due to spatial heterogeneity. Therefore, an optimal method to estimate the actual temperature from mixed land-use types in a pixel of Landsat-8 data has yet been examined and criticized. This study aimed to explore the optimum method in LST estimation over four favoured algorithms, RTE, IMW, GSC, and SW, regarding their widely use in these recent years. As a result, the four LST retrieval algorithms were criticized and explored the limits of the applied parameters. This study is beneficial to the GIS specialists working for local government to follow the best practice for the LST estimation over a city. Later, provincial officers can use the explored results from the optimal method to monitor the LST over a small and diverse city, as Buriram Town Municipality.

2. Theories and concepts

2.1 Land Surface Temperature (LST) estimation

There are four LST (Land Surface Temperature) estimation algorithms typically employed in these recent decades in response to the remote sensing data. The RTE and IMW were developed by Wang *et al.* [17]. The GSC and SW were developed by Jimenez-Munoz *et al.* [18]. The first one, Radiative transfer equation-based method (RTE), was developed by Wang *et al.* [17] with the concern of radiative transfer equation based on Plank's law inversion [19]. The atmospheric profile was extracted from the NCEP (National Centers for Environmental Prediction) dataset and used to simulate atmospheric transmittance, up-welling, and down-welling radiance from the Moderate-resolution atmospheric Transmission (MODTRAN) model [11]. The expression of the RTE is,

$$LST = \frac{C_2}{\lambda \ln\left\{\frac{C_1}{\lambda^5\left[\frac{L_{sensor} - L_u - \tau(1-\varepsilon)L_d}{\tau\varepsilon}\right]} + 1\right\}} \tag{1}$$

Where L_{sensor} is thermal radiance at the sensor level, ε is land-surface emissivity, τ is atmospheric transmissivity, L_u and L_d are up-welling and down-welling atmospheric radiance, respectively, and C_1 and C_2 are the constant-coefficients.

Later, Qin *et al.* [20] developed the mono-window algorithm. It was used for estimating the LST from LANDSAT-5 to avoid dependence on radio-sounding in the RTE method [21]. Consequently, Wang, *et al.* [17] developed the mono-window into the Improved Mono-Window (IMW) method for obtaining LST from LANDSAT-8 in 2015 [11], as shown in the following expression.

$$LST = \frac{1}{C}[a(1 - C - D) + (b(1 - C - D) + C + D)T_B - DT_a] \tag{2}$$

$$\text{With } C = \varepsilon\tau$$

$$D = (1 - \tau)[1 + (1 - \varepsilon)\tau]$$

Where a and b are constant coefficients, ε is the land surface emissivity, τ is the total atmospheric transmissivity, T_B is the at-sensor brightness temperature, and T_a is the mean atmospheric temperature.

In 2003, Jimenez-Munoz and Sobrino [22] initially developed the Generalized Single-Channel (GSC) algorithm to estimate the LST from LANDSAT-5. It was further developed in 2014 to obtain LST from LANDSAT-8, shown in the following expression [11].

$$LST = \gamma\left[\varepsilon^{-1}\left(\psi_1 L_{sensor} + \psi_2\right) + \psi_3\right] + \delta \tag{3}$$

$$\text{With } \gamma = \frac{T_B^2}{b_\gamma L_{sensor}} \quad (4)$$

$$\delta = T_B - \frac{T_B^2}{b_\gamma} \quad (5)$$

Where L_{sensor} is thermal radiance at the sensor level, b_γ equals 1,324 K, and 1,199 K for TIRS-1 (Band 10) and TIRS-2 (Band 11), respectively, T_B is at-sensor brightness temperature, ε is the land surface emissivity, and ψ_1, ψ_2, ψ_3 can be obtained as a function of the total atmospheric water vapor content (w).

Eventually, the split-window algorithm, developed by Jimenez-Munoz, *et al.* [18] is shown in the following expression.

$$T_s = T_i + C_1(T_i - T_j) + C_2(T_i - T_j)^2 + C_0 + (C_3 + C_4 w)(1-\varepsilon) + (C_5 + C_6 w)\Delta\varepsilon \quad (6)$$

Where C_0 to C_6 are the split window coefficients, T_i and T_j are at-sensor brightness temperature of Band i and j, respectively, ε is the land surface emissivity obtained from $\varepsilon = 0.5\ (\varepsilon_i + \varepsilon_j)$ and $\Delta\varepsilon = (\varepsilon_i - \varepsilon_j)$.

It is noted that the near-surface air temperature (T_0) and relative humidity were received from Huai Rat Station near Buriram Town Municipality (approximately twelve kilometers). As mentioned in a report of Salakkham and Piyatadsananon that near-surface air temperature (T_0) and relative humidity can be found on the Hydro and Agro Informatics Institute (HAII) website [11]. The parameters were used in the water vapor content calculation and estimation developed by Liu and Zhang [23], as equation (7). The water vapor content has been used in the transmittance calculation for the IMW algorithm, the atmospheric function, the GSC algorithm, and the SW algorithm [11]. This parameter has also been used in the atmospheric temperature (T_a) calculation, an essential parameter of the IMW algorithm.

$$w_i = \left\{0.59 \times RH \times exp\left[\frac{17.27 \times (T_0 - 273.15)}{237.3 + (T_0 - 273.15)}\right]\right\} + 0.1697 \quad (7)$$

Where w_i is the water vapor content (g cm^{-2}), T_0 is the near-surface air temperature (K), and *RH* is the relative humidity (Decimal). The water vapor content, near-surface air temperature, and relative humidity are the average values.

The transmittance, up-welling, and down-welling atmospheric radiance were obtained from the NASA atmospheric correction parameter calculator [11]. It is clearly shown that the calculator uses the National Centers for Environmental Prediction (NCEP) to model global atmospheric profiles, which are interpolated to a particular date, time, and location as input for the MODTRAN radiative transfer code, and as a suite of the integrative algorithm to infer the up-welling, down-welling radiances and site-specific transmission [11]. The profiles resulting from time interpolation provide the closet latitudinal and longitudinal positions or specific locations [24].

3. Methods

3.1 Study Area

Buriram province is located in the Northeastern region of Thailand. It has flourished over the last decade as a sports city of the country. A mega-sports complex, which contains a massive stadium for football, a motor racing track, and several ongoing construction projects, attracts many tourists and drives up the demand for further construction across Buriram Town Municipality [25], [26]. The local government has planned to improve the Town Municipality to City Municipality to support the urbanization [25]. As six square kilometers for over 30,000 families living in the municipality, Buriram municipality is the most crowded city (around five-thousand population in a square kilometer) in the Northeastern region [27]. The maximum temperature in the summer has increased to more than 40 °C (in 2013 – 2018) [28].

3.2 Data collection

The data used in the LST estimation of this study are listed in table 1 with their sources.

Table 1. Data used in the study.

Data	Date	Sources
LANDSAT-8 data Path /Row: 128 /50	Jan 21st, Feb 6th, Mar 26th, Apr 11th, 2018	U.S. Geological Survey (USGS)
UAV image (GSD = 5cm.)	Mar – Apr, 2018	Surveying between 10-11 am.
Ground-based temperature data	Jan 21st, Feb 6th, Mar 26th, Apr 11th, 2018	Surveying between 10-11 am.
Atmospheric parameters • Air temperature • Relative humidity	Jan 21st, Feb 6th, Mar 26th, Apr 11th, 2018 Between 10-11 am.	Hydro and Agro Informatics Institute (HAII) website
Atmospheric parameters • Transmittance • Up-welling and down-welling atmospheric radiance	Jan 21st, Feb 6th, Mar 26th, Apr 11th, 2018	NASA atmospheric correction parameter calculator website

The atmospheric parameters used in the LST estimation of four methods are listed in table 2.

Table 2. Atmospheric parameters used in LST estimations.

		Jan 21st	**Feb 6th**	**Mar 26th**	**Apr 11th**
Temperature (T_0) (K)		303.9	293.1	302.9	309.3
Air Temperature (T_0) (°C)		30.75	19.95	29.75	36.15
Relative Humidity		0.63	0.60	0.65	0.44
Water Vapor Content		2.86	1.52	2.79	2.72
Methods	**Atmospheric Parameters**	**Jan 21st**	**Feb 6th**	**Mar 26th**	**Apr 11th**
RTE	Transmittance (τ) ^{a}	0.53	0.80	0.54	0.60
	Up-welling	3.92	1.63	3.78	3.56
	Down-welling	6.00	2.67	5.86	5.65
IMW	Atmospheric Temperature (T_a)(K)	296.69	286.79	295.78	301.65
	Transmittance (τ) ^{b}	0.65	0.80	0.65	0.65
GSC	Atmospheric Function (ψ_1)	1.42	1.15	1.41	1.39
	Atmospheric Function (ψ_2)	-7.25	-2.97	-6.99	-6.70
	Atmospheric Function (ψ_3)	3.69	1.81	3.60	3.49
SW	Water Vapor Content	2.86	1.52	2.79	2.72

Note: ^{a} Transmittance, up-welling, and down-welling used in the RTE method were obtained from NCEP
^{b} The transmittance used in IMW was calculated based on the mono-window method.

3.3 Procedures

The conceptual procedure of this study is illustrated in figure 2. It consists of three major parts, (1) ground-based temperature measurement, (2) LST estimation, and (3) the comparison between ground-based temperature data and the calculated LST data from the Landsat 8 data. Eventually, the optimum method of LST estimation was then identified by considering the lowest calculated NRMSE values.

3.3.1 Ground-based temperature measurement

Basically, the LANDSAT-8 image contains 30x30 meter-grids, whereas the thermal band image consists of 100x100 meter-grids. Therefore, an aggregated pixel of 3x3 pixels (90x90 m.) of OLI was assembled to be a pixel size of the Thermal image (100x100 m.). The Land-Use and Land-Cover (LULC) types, within a thermal pixel (100x100 m.) were classified by visual interpretation technic on the high-resolution image from UAV. The LULC within a thermal grid cell was assessed the weighted value regarding the proportion of the mixed LULC. The high-resolution image from UAV was also used as the based map for planning the ground-based temperature measurement. A hand-held digital thermometer was calibrated every time before measuring the LST in the sample sites. One hundred sample sites were measured and recorded the land surface temperature in the center of the 3x3 pixels of OLI, or 90x90 m. of thermal bands during 10-11 am. on Jan 21st, Feb 6th, Mar 26th, and Apr 11th, 2018.

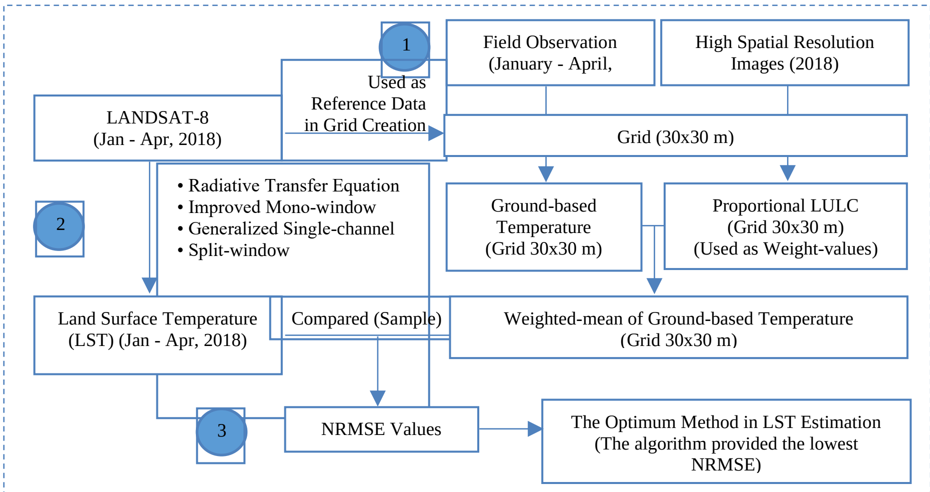

Figure 1. The conceptual procedure of the study

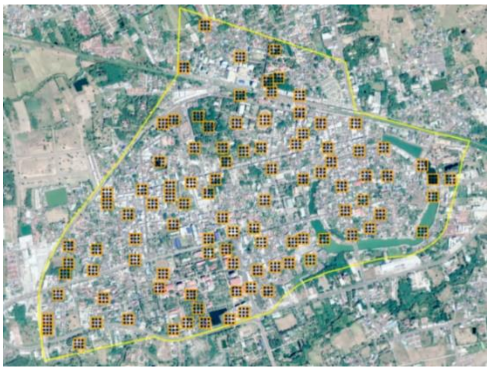

Figure 2. The 100 sample sites (small orange grids) over Buriram Municipality (yellow boundaries)

3.3.2 Accuracy assessment

The optimum method in the LST extraction, RTE, IMW, GSC, and SW algorithm, as equation (1) – (7), were used in the calculations. Eventually, the method in which provides the lowest NRMSE values considers as an optimum method of the LST estimation of Buriram Town Municipality.

$$NRMSE = \frac{RMSE}{maximum\ observation - minimum\ observation} \tag{8}$$

Where *maximum* and *minimum* observations are the maximum and minimum temperature of in-situ data.

4. Results and Discussion

The result from split-window technique shows more complex surface than others (in figure 3). As a reason, two thermal infrared channels have narrower bandwidths, which can capture finer land surface information response to studies of Li, *et al.* [29] and Du, *et al.* [30]. The accuracy assessment was examined to explore the optimum method in the LST estimation by considering the lowest NRMSE value of each method. The RMSE and NRMSE values, as shown in table 3 and figure 4. The SW method eliminates atmospheric effects based on differential absorption in two thermal bands, which have narrow bandwidths in the thermal infrared [11]. As supported by the studies of Caselles *et al.* [31] and Rozenstein *et al.* [32], whether two separating narrow thermal infrared presents the smallest error in the

LST retrieval. However, the SW algorithm is sensitive to water vapor content and coefficients. Typically, the coefficients used in the SW algorithm are based on the series of studies of Jimenez-Munoz *et al.* [18], [33, 34]. In addition, the coefficients depend on the atmospheric state, while the fixed values were sometimes utilized, causing significant errors to the results, as highlighted in a study by Vazquez *et al.* [35].

Table 3. NRMSE Values of the LST estimation methods

Date	NRMSE			
	RTE	**IMW**	**GSC**	**SW**
Jan 21st, 2018	0.454	0.613	0.650	0.227
Feb 6th, 2018	0.702	0.317	0.671	0.473
Mar 26th, 2018	0.246	0.416	0.509	0.218
Apr 11th, 2018	0.165	0.226	0.202	0.132
Overall NRMSE	0.171	0.181	0.219	0.114

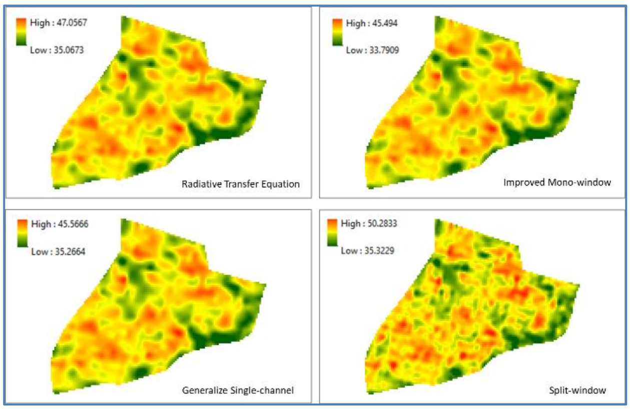

Figure 3. LST calculated by four methods

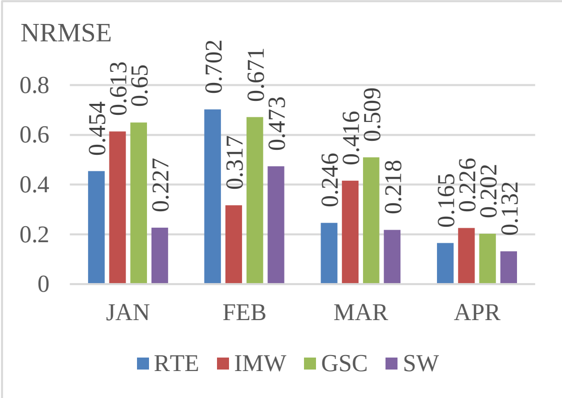

Figure 4. NRMSE values, monthly results.

On the other hand, the single-channel methods, RTE, IMW, and GSC algorithms, rely on the accuracy of the radiative transfer model and the atmospheric profiles representing the actual state of the atmosphere over the studies area at the orbital time [11]. The error of the RTE algorithm comes from the atmospheric model used in the calculation of the atmospheric parameters. Since the study area is located in the tropical zone, the available model is the NCEP model presenting the mid-latitude summer and mid-latitude winter models, as same as the discussion in a study of Jimenez-Munoz *et al.* [36]. The error from the IMW algorithm comes from the essential atmospheric parameters used in this algorithm. There is no reference source in near-ground air temperature (T_0) acquisition, which is used in the sufficient atmospheric temperature (T_a). The sufficient atmospheric temperature (T_a) is an essential practical issue used to retrieve LST over a large area, as emphasized by Cristobal, *et al.* [37]. Lastly, the GSC algorithm provides a higher error than other methods. The basis of this algorithm relies on the estimation of the so-called atmospheric function, which is assumed to be dependent only on water vapor content values [11]. As the studies of Chen, *et al* and Cristobal *et al.* [37], [38] explained that the atmospheric functions might be obtained more precisely from water vapor content and air temperature.

5. Conclusion

It can be concluded that the SW algorithm provided the lowest NRMSE value (0.114); nevertheless, the IMW algorithm provided a better result than the SW algorithm on Feb 6th 2018. It is noticeable that the average temperature on Feb 6th 2018 was dramatically dropped to 19.95 ºC, shown in table 2, so that it caused the lowest water vapor content (1.52 g cm^{-2}) in Feb 2018. For this reason, the critical point is that the amount of atmospheric water vapor content data plays an essential role in calculating accuracy. This parameter is typically estimated by considering the near-surface air temperature and relative humidity values [11]. In order to enhance the accuracy of all practiced algorithms, it is recommended to obtain the near-surface air temperature and relative humidity in-situ of the study area. Apart from the atmospheric correction parameters, the surface emissivity must also be considered to enhance the accuracy of the LST retrieval. The study area, Buriram Town Municipality, appears as heterogeneous LULC within a thermal-image pixel, causing different reflectance of the spectrum. Regarding coarse spatial resolution, it is strongly affected by mixed pixels, whereby each pixel comprises a mixture of two or more land cover types [39]. Therefore, the SW algorithm is recommended for the LST estimation in a small city, like Buriram municipality. It can be done regularly using the Landsat-8 data with sub-pixel technique, which can monitor the LST in small cities. Considering the limitation of the parameters used in the SW method, it is suggested that a local weather station in the city should be identified to provide the near-surface air temperature and relative humidity values. The explored optimum method for the LST estimation from this study will be useful to GIS specialists, who are working for the local government to conduct this technic to prevent the urban heat island (UHI) in small cities with similar contents.

References

[1] Holmes TRH, Crow WT, Yilmaz MT, Jackson TJ and Basara JB 2013 *Journal of Geophysical Research: Atmospheres,* **118** 577

[2] Wu P, Shen H, Ai T and Liu Y 2013 *International Journal of Digital Earth* **6** 113

[3] Orhan O, Ekercin S and Dadaser-Celik F 2014 *The Scientific World Journal* **2014** 1

[4] Weng Q and Fu P 2014 *Remote Sensing of Environment* **140** 267

[5] Wu P, Shen H, Zhang L and Gottsche F-M 2015 *Remote Sensing of Environment* **156** 169

[6] Weng Q, Fu P and Gao F 2014 *Remote Sensing of Environment* **145** 55

[7] Avdan U and Jovanovska G 2016 *Journal of Sensors* **2016** 1

[8] Bendib A, Dridi H and Kalla MI 2017 *Geocarto International* **32** 503

[9] Mechri R, Ottle C, Pannekoucke O and Kallel A 2014 *Journal of Geophysical Research: Atmospheres* **119** 2131

[10] Zhou J, Dai F, Zhang X, Zhao S and Li M 2015 *International Journal of Applied Earth Observation and Geoinformation* **34** 35

[11] Salakkham E and Piyatadsananon P 2020 Suranaree University of Technology, Seminar Report.

[12] Jimenez-Munoz J C, Sobrino JA, Skokovic D, Matter C and Cristobal J 2014 *IEEE Geoscience and Remote Sensing Letters* **11** 1840

[13] Li ZL, Tang BH, Wu H, Ren H, Yan G, Wan Z, Trigo IF and Sobrino JA 2013 *Remote Sensing of Environment* **131** 14

[14] Weng Q, Lu D and Schubring J 2004 *Remote Sensing of Environment* **89** 467

[15] Liu Y, Hiyama T and Yamaguchi Y 2006 *Remote Sensing of Environment* **105** 115

[16] Coll C, Galve JM, Sanchez JM and Caselles V 2010 *IEEE Transactions on Geoscience and Remote Sensing* **48** 547

[17] Wang F, Qin Z, Song C, Tu L, Karnieli A and Zhao S 2015 *Remote Sensing* **7** 4268

[18] Jimenez-Munoz J C, Sobrino J A, Skokovic D, Matter C and Cristobal J 2014 *IEEE Geoscience and Remote Sensing Letters* **11** 1840

[19] Skokovic D *et al.* 2014. [Online]. Available: https://earth.esa.int/documents/700255/2126408/ESA_Lpve_Sobrino_2014a.pdf

[20] Qin Z, Karnieli A and Berliner P 2001 *International Journal of Remote Sensing* **22** 3719

[21] Sobrino JA, Jimenez-Munoz JC and Paolini L 2004 *Remote Sensing of Environment* **90** 434

[22] Jimenez-Munoz J C and Sobrino JA 2003 *Journal of Geophysical Research* **108** 1

[23] Liu L and Zhang Y 2011 *Remote Sensing* **3** 1535

[24] Vlassova L, Perez-Cabello F, Nieto H, Martin P, Riano D and Riva J d l 2014 *Remote Sensing* **6** 4345

[25] Buriram World https://www.buriramworld.com/ (accessed Jul., 2017)

[26] Tourism Authority of Thailand https://www.tourismthailand.org/About-Thailand/Destination/Buri-Ram (accessed Jul., 2017)

[27] The Bureau of Registration Administration http://stat.bora.dopa.go.th/stat/statnew/statTDD/ (accessed Nov., 2018)

[28] Buriram Statistic Office http://buriram.old.nso.go.th/nso/project/search_option/search_result.jsp (accessed Jan, 2021

[29] Wenbin L, Yonghua S, Dan M and Xiaojuan L 2013 *IEEE International Geoscience and Remote Sensing Symposium*
[30] Du C, Ren H, Qin Q, Meng J and Zhao S 2015 *Remote Sensing* **7** 647
[31] Caselles V, Rubio E, Coll C and Valor E 1998 *Journal of Geophysical Research* **103** 17057
[32] Rozenstein O, Qin Z, Derimian Y and Karnieli A 2014 *Sensors* **14** 5768
[33] Jimenez-Munoz JC and Sobrino JA 2008 *IEEE Geoscience and Remote Sensing Letters* **5** 806
[34] Jin M, Li J, Wang C and Shang R 2015 *Remote Sensing* **7** 4371
[35] Vazquez DP, Reyes FJO and Arboledas LA 1997 *Remote Sensing of Environment* **62** 215
[36] Jimenez-Munoz JC, Cristobal J, Sobrino JA, Soria G, Ninyerola M and Pons X 2009 *IEEE Transactions on Geoscience and Remote Sensing* **47** 339
[37] Cristobal J, Jimenez-Munoz JC, Sobrino JA, Ninyerola M and Pons X 2009 *Journal of Geophysical Research,* **114** D08103
[38] Chen F, Zhao X, Ye H and Hu H 2011 Spatial Data Mining and Geographic Knowledge Services (ICSDM), Fuzhou, China
[39] Feng X, Foody G, Aplin P and Gosling SN 2015 *Sustainable Cities and Society* **19** 341